Photometric Analysis of Three Prominent Stella Clusters; Messier 2 (NGC 7089), Beehive Cluster (NGC 2632), and Tarantula Nebula Cluster (NGC 2070)

Physics Department, University of California, Santa Barbara, CA 93106-9530

(Dated: December 1, 2022)

Abstract

A photometric analysis of three different star clusters was produced from data obtained by the Las Cumbres Observatory (LCO) 0.4 m telescope: Messier 2 – NGC 7089, one of the oldest and largest MW globular clusters; the Beehive Cluster (Praesepe) – NGC 2632, a well populated, nearby open cluster of intermediate age; and NGC 2070 at the center of Tarantula Nebula, a very massive, very young open star cluster. Images were obtained in all filter bands from UV to Infrared, and analyzed with aperture photomtry using Photutils in Python. Color Magnitude diagrams were produced in U-B, B-V, V-R, and R-I, then compared with published color magnitude diagrams for each cluster. Estimates of main sequence populations were made. Results indicate a less well populated upper main sequence for Messier 2 (NGC 7089), consistent with estimated age of 13 Gyr; a well populated entire main sequence for Beehive Cluster (NGC 2632), consistent with estimated age of 900 Myr; and inconclusive results for NGC 2070 due to unsatisfactory signal to noise and telescope constraints.

INTRODUCTION

The Hertzsprung-Russell Color-Magnitude Diagram

The Hertzsprung-Russell diagram, so fundamental to astrophysical theory, illustrates the many relationships between physical parameters of stars and offers us a powerful tool for understanding the varied populations of stars that we observe in the sky as well as their evolutionary paths as they burn through their nuclear fuel. The primary structure of the H-R diagram rests on the relationship between the 'color' of a star, and its 'brightness', or magnitude. This 'color-magnitude' relationship can be more fundamentally understood as a 'Luminosity-Temperature' relationship. When plotting the absolute magnitude (or luminosity) on the vertical axis, and a measure of the color (temperature) on the horizontal axis, a clear inverse linear relationship is illustrated.

Historical Background

This first H-R diagram (Figure 1. above) was produced in 1914 by the American astronomer, Henry Russell (1877-1957). Both Russell and Danish astronomer, Ejnar Hertzsprung (1873-1976), analyzed stars within a particular spectral type (color, temperature) and noticed that within that spectral type there was a large range of absolute magnitudes (luminosities). Using a version of the Stefan-Boltzmann equation which relates temperature, radius and luminosity of spherical stars,

$$R = \frac{1}{T_eff}\sqrt{\frac{L}{4\pi\sigma}} \tag{1}$$

it could be shown that the radii of stars (their "size') can be determined from their temperature and luminosity. Russell termed the larger stars 'giants' and the smaller ones 'dwarfs' (Carroll and Ostlie 2017). When the horizontal and vertical axes use a logarithmic scale the range of stella sizes fit largely in a neat band running diagonally from top left to bottom right, termed the 'main sequence', with giant stars above the band and dwarf stars below it. Lines of constant radius can also be plotted, and they run roughly diagonally too. These relationships together lead to the conclusion that position on the main sequence is essentially determined by stella mass. The Figure 1b. above shows a modern 'color-magnitude' diagram derived from about 3000 stars, while Figure 1c. shows a theoretical 'luminosity-temperature' diagram derived from stella spectral theory (Carroll and Ostlie 2017).

In 1956 Merle Walker used the tri-color photoelectric UBV system to produce color magnitude diagrams for a very young star cluster, NGC 2264, with an estimated age of approximately 3 million years. Walker points out the challenges of getting accurate color-magnitude diagrams of young clusters: stars need to be in a clear group association; they must contain both massive, bright stars, and low mass faint stars (nearby clusters allow both); there must be minimum emission nebulosity (or you can't see the faint stars); and preferably a small, uniform interstellar reddening (Walker 1956).

In this report we detail a UBVRGI photometric analysis of three stella clusters Messier 2 (NGC 7089), one of the oldest and largest Milky Way globular clusters; the Beehive Cluster (Praesepe - NGC 2632) a well populated, Milky Way open cluster of intermediate age; and NGC 2070 at the center of Tarantula Nebula in the Large Magellanic Cloud, a very massive, extremely young, open star cluster.

Theory

Stella Brightness

The Inverse Square Law for light tells us that the energy of electromagnetic radiation reduces as the square of its distance from us This fundamental property of light allows us to relate measured quantities from stars, like apparent magnitude (m) and radiant flux, (F) to intrinsic properties of those stars, absolute magnitude (M) and luminosity (L), by using the Sun as a reference value:

$$M = M_{Sun} - 2.5\log_{10}\left[\frac{L}{L_{Sun}}\right] \tag{2}$$

$$m = M_{Sun} - 2.5\log_{10}\left[\frac{F}{F_{Sun(at 10 parsecs)}}\right] \tag{3}$$

A star's brightness is measured by the amount of electromagnetic energy received at a detector (radiant flux F in Wm-2) which is some distance from the star. This apparent magnitude of the star is related to its absolute magnitude by the distance, via the distance modulus equation:

$$m - M = 5\log_{10}\left[\frac{distance}{10\ parsecs}\right] \tag{4}$$

If we know the distance to a star, say from parallax measurements, then we can apply the distance modulus relationship to determine its absolute magnitude, and its luminosity (Carroll and Ostlie 2017).

Peak Wavelength and Color Indices

We can think of stars as near perfect blackbody radiators, where all the light coming from the star is due entirely to processes in the star. Blackbody radiation is a continuous spectrum with some energy at all wavelengths, but there will always be a 'peak wavelength', λ_{max}, which supplies most of the energy. This λ_{max} produces the primary color of the star, and it is different for each type of star. There is a fundamental relationship between this λ_{max} (color) and the Temperature of the star, which is described by Wien's displacement law $\lambda_{max}T = 0.002898\ mK$. Thus, by determining the peak wavelength from a star, we may infer its effective surface temperature, T_{eff} (Carroll and Ostlie 2017). A detailed spectral line analysis for each star of the cluster would provide the effective temperature for that star, but there is a quicker way, especially for clusters with many stars.

To determine the peak wavelength, astronomers measure the electromagnetic flux when particular 'filters' are applied to the detector. These filters transmit the light only within certain narrow wavelength regions, or 'bands'. This allows us to determine the magnitude in a particular band (ie. M_{UV}, M_{Blue} , $M_{Visible}$). By subtracting two neighboring band magnitudes, (ie. $M_{UV} - M_{Blue}; or\ M_{Blue} - M_{Visible}$), we achieve a 'color index' (eg. U-B, or B-V). Color indices allow us to objectively determine a stars color, and therefore effective temperature, which we can then use to determine other characteristics of the star, such as size, mass, and age (Lubin 2022; Carroll and Ostlie 2017).

Stella Evolution and The HR Diagram

Stars form as an overdense region of interstellar gas begins to contract under gravity. The gas cloud does not contract uniformly to a central point, but rather it contracts radially in several regions, encompassing different masses of gas. As such stars form in 'clusters', with a range of different masses. This range of masses is a fundamental property of the cluster and is known as the initial mass function of the cluster (distribution of stars in each mass range). The initial mass function is responsible for many of the characteristics of the cluster. The result of this model of star formation is that the stars in a cluster all have roughly the same composition, age, and distance from us. It then follows that the key distinguishing factor for differences between the stars in the cluster is mass (Voyt-Russell Theorem)(Carroll and Ostlie 2017).

Stars of different masses evolve in different ways, indicated by their 'evolutionary tracks' (Isochrones). Stars have 'pre-main sequence tracks', which indicate where stars sit on the HR, before they get to the main sequence, and 'post-main sequence tracks', which indicate where they sit on the HR after they leave the main sequence. If we can observe a star at a particular position on a HR diagram, we can infer an approximate age for that star (Carroll and Ostlie 2017).

Turn Off Points in Color Magnitude Diagrams

The theoretical 'zero age' main sequence (ZAMS) describes a very young cluster where the stars are only just beginning their nuclear fusion processes in the core of the stars. The main sequence will have larger mass, hotter, brighter stars in the upper left corner running smoothly, diagonally, down to smaller, dimmer, lower mass stars at the bottom right. As the cluster ages, the more massive stars in the top right, burn through their fuel quicker, and burn out. This leads to an older cluster having no stars in that upper left corner, but some cooler supergiants will be appearing in the upper right. As clusters continue to age, we see many more stars 'turning off' the main sequence, and evolving toward the red giant section. Eventually, all the main sequence stars are gone, and we are left with mostly old, cooler, red stars of intermediate size (Richmond, no date.).

A color-magnitude plot of most of the stars in the cluster, will reveal the location of this main sequence 'turn off point', where stars are leaving the main sequence, becoming redder and less bright. The location of the turn off point can then be used to estimate the age of the cluster (Carroll and Ostlie).

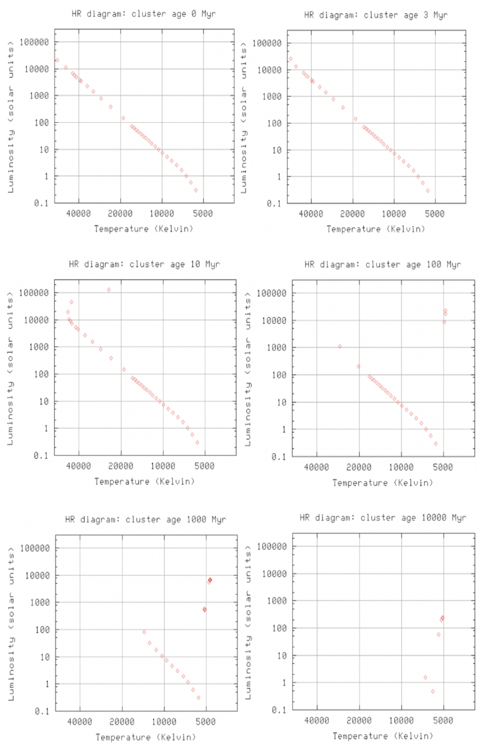

FIG. 1: HR Diagrams at Different Ages: (0 to 10 Billion years)

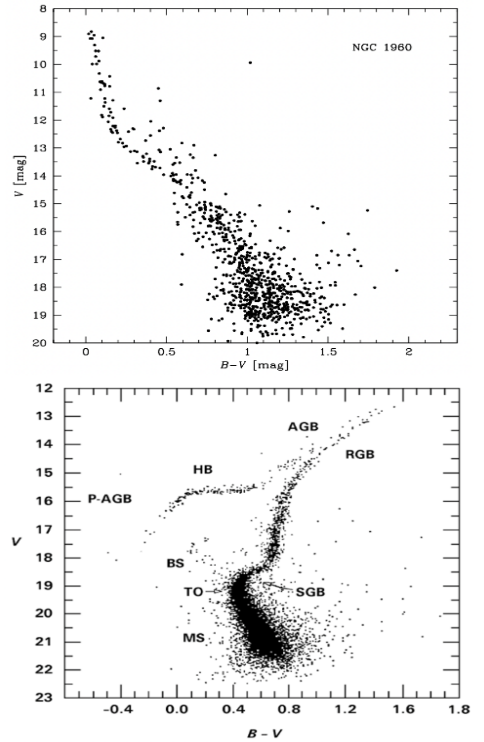

FIG. 2: Top:Young Cluster. Bottom: Old Cluster

FIG. 3 above displays theoretical HR Diagrams at different Ages (0 to 10 Billion years). These HR diagrams illustrate higher mass stars leaving the main sequence and migrating to the giant sub branches. The theoretical main sequence turn off points are used to compare with color-magnitude diagrams to estimate the age of a cluster (Richmond, no date). FIG. 4 above (Top panel) displays color magnitude diagram of NGC 1960, a young, open cluster (25 Myr)(Sanner 2000); FIG.4 (Bottom Panel) displays a color magnitude diagram of Messier 3, an old globular cluster (11.5 Gyr)(Carroll and Ostlie 2017).

Larger context of Importance of the Research

Detailed age analysis of star clusters provides a link between theory and observation allowing the necessary fine tuning of theoretical models. The study of very old (10-14Gyr) globular clusters assists in developing theories of galactic evolution (de Brito Silva et al. 2022), while the study of young clusters contributes to theories of stella evolution and mass functions

(Lodieu 2019).

While photometric analysis gives us a relatively simple inexpensive procedure for obtaining an overall picture of the population of stars in the cluster, modern methods of stella spectral analysis allow us to take a detailed spectrum of a star, determine its spectral class, and find its place directly on the H-R diagram. We can then read off its absolute magnitude from the vertical axis. This is powerful because it allows us to infer a distance, it's 'spectroscopic parallax'.

$$distance\,(pc) = 10^{\frac{(m-M+5)}{5}} \tag{5}$$

By performing spectral analysis on many of the individual stars in a star cluster, all essentially at the same distance, we multiply the robustness of these distance estimates.

METHOD

TABLE I: Star Cluster Location, Distance, and Apparent Magnitude in the Visible

Star Cluster	Constellation	Distance(ly)	Apparent Magnitude (mv)
Messier 2 – NGC 7089	Aquarius	55,000	6.5
Beehive Cluster (Praesepe) – NGC 2632	Cancer	600	3.7
Center of Tarantula Nebula - NGC 2070	Dorado	160,000	8

Data Collection

Data was obtained from Las Cumbres Observatory (LCO) between mid-October and mid-November 2022, using their SBIG 6303 0.4 m telescope in 3k x 2k format. The CCD (KAF-6303E/LE) images were obtained in 6 different filters: Bessel Blue; Bessel Visible; SDSS Ultraviolet; SDSS Green; SDSS Red; and SDSS Infrared (see Table II below for specifications). Ten images with integration time of 5 seconds each were obtained for each of the 6 filters. 60 Images in total. Output formats of images were in .fits files.

TABLE II: Telescope and CCD Specifications

Read Noise (NR)	13.5	Pixel Size (Ω)	0.326 arcsec^2
Dark Current (iDC)	0.3 @ T=0deg	Telescope Area (A)	1257 cm^2
Quantum Efficiency (Qe)	68%	Telescope Efficiency (ϵ)	0.5

Data Analysis

The images where processed in both AstroArt, to stack images and create final tricolor images; as well as Python in Jupyter Notebooks, to create Color-Magnitude diagrams. Photutils package was used for estimating and subtracting off background, detecting point sources, and applying aperture photometry (see Appendix A Python Script for details).

RESULTS

Summary Images

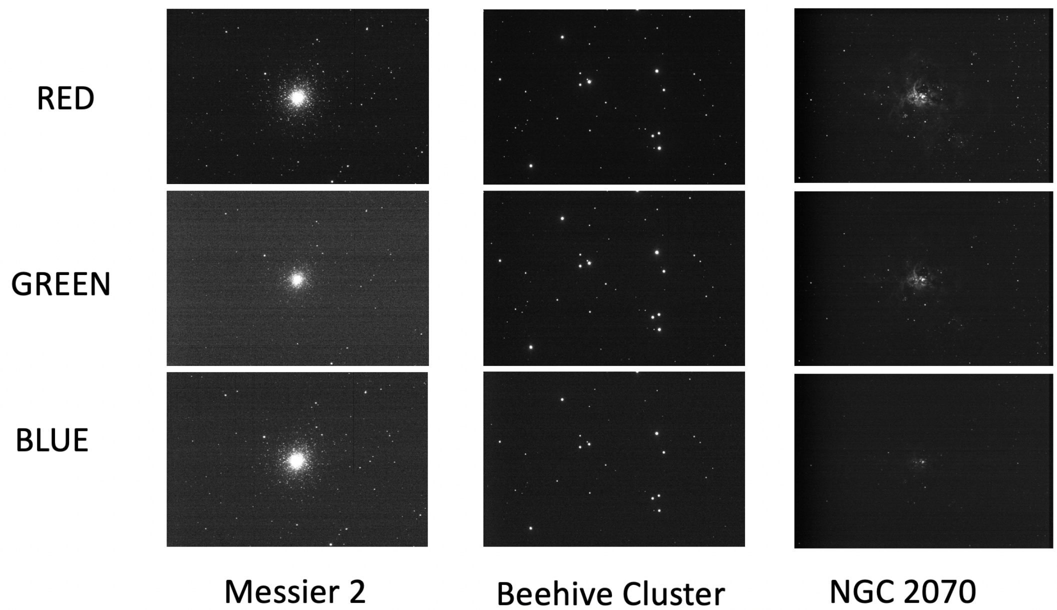

FIG. 3: Base Images: Raw base images with a 5 second integration time in each filter were stacked (10 images) in AstroArt, to produce final Red, Green and Blue base images for Messier 2, the Beehive Cluster, and NGC 2070.

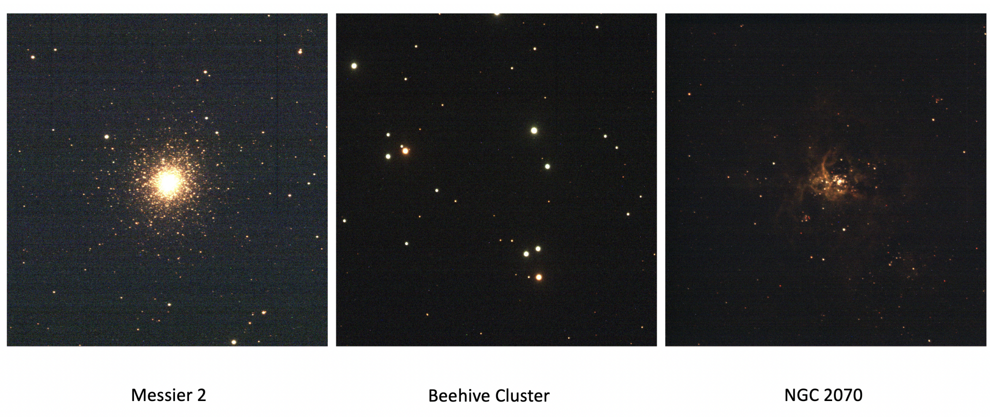

FIG. 4: Tricolor Images: Final RGB Tricolor Images produced in AstroArt from red, green and blue base images for Messier 2, the Beehive Cluster, and NGC 2070.

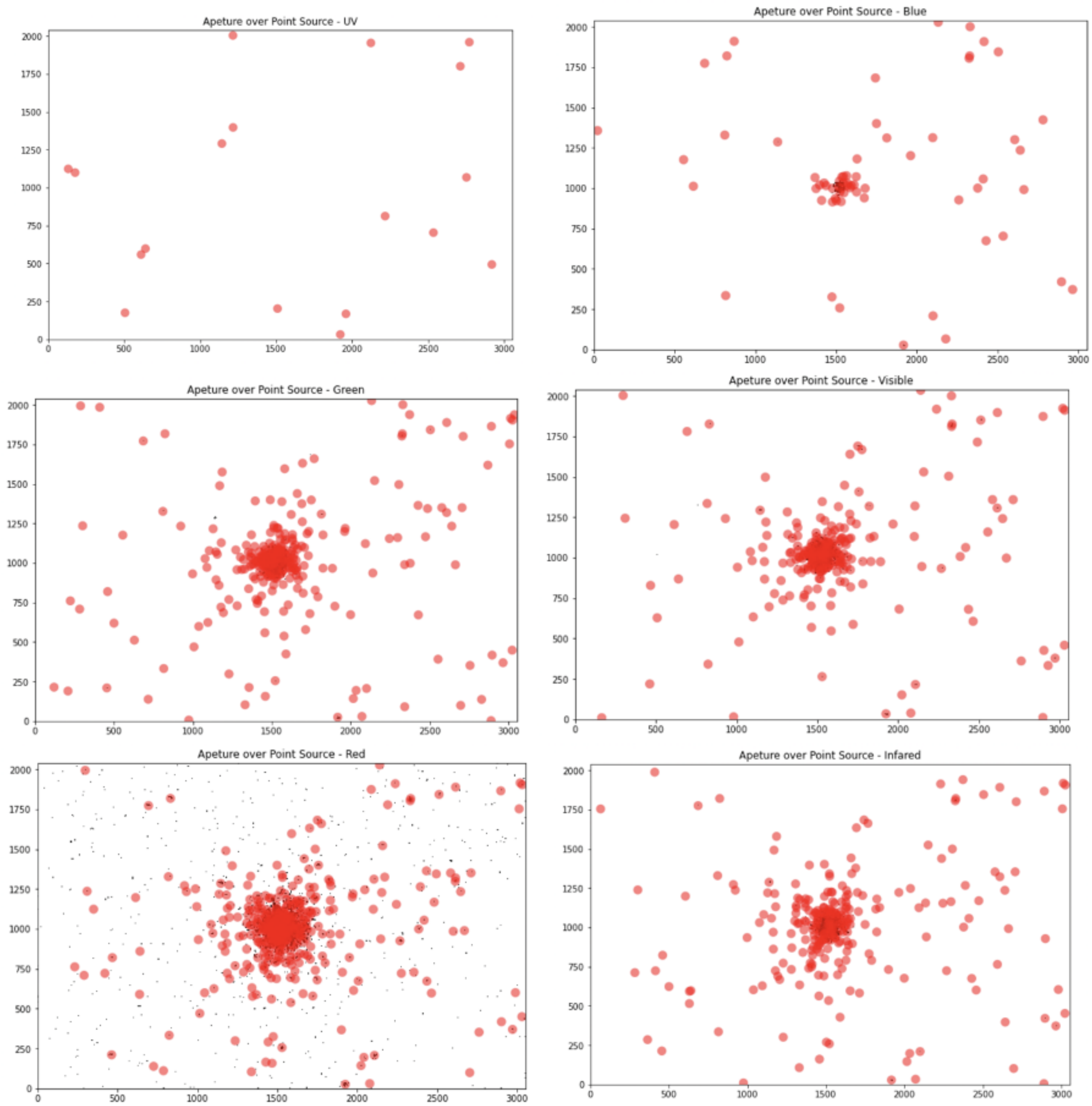

FIG. 5: Messier 2 Aperture Photometry Plots:

Aperture Over Point Sources Detected in six different filter bands: From left to right, top to bottom; Bessel UV; Bessel Blue; SDSS Green; SDSS Visible: SDSS Red; and SDSS Infrared. Most of the point sources detected for Messier 2 are in the red band, with a significant number in the infrared and green. Far fewer are detected in the blue; and only very few in the UV.

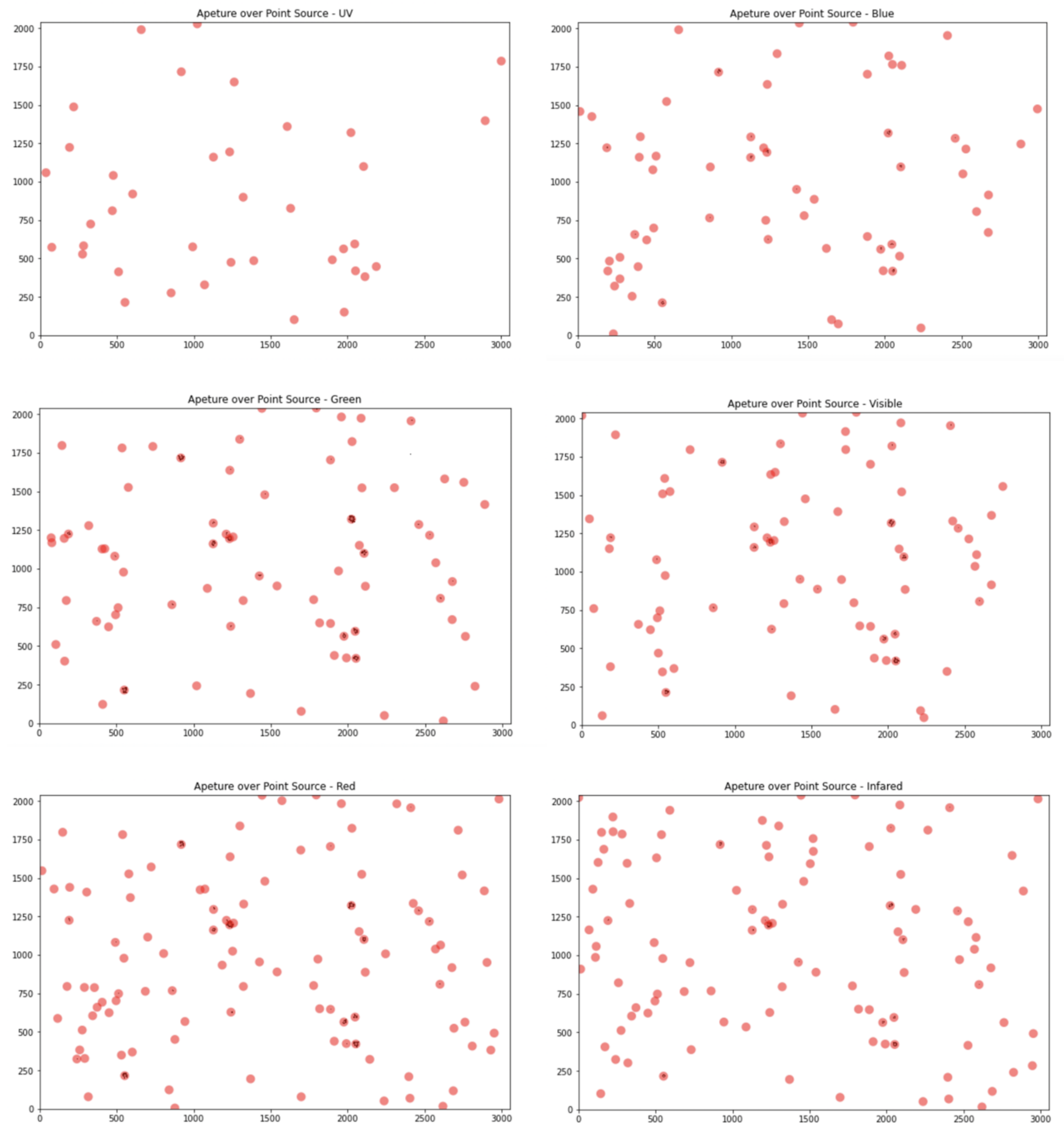

FIG. 6: Beehive Cluster Aperture Photometry Plots:

Aperture Over Point Sources Detected in six different filter bands: From left to right, top to bottom; Bessel UV; Bessel Blue; SDSS Green; SDSS Visible: SDSS Red; and SDSS Infrared. Point sources were detected in each of the six bands, with green, red, and infrared sources slightly dominating the blue sources, and with fewer UV sources detected.

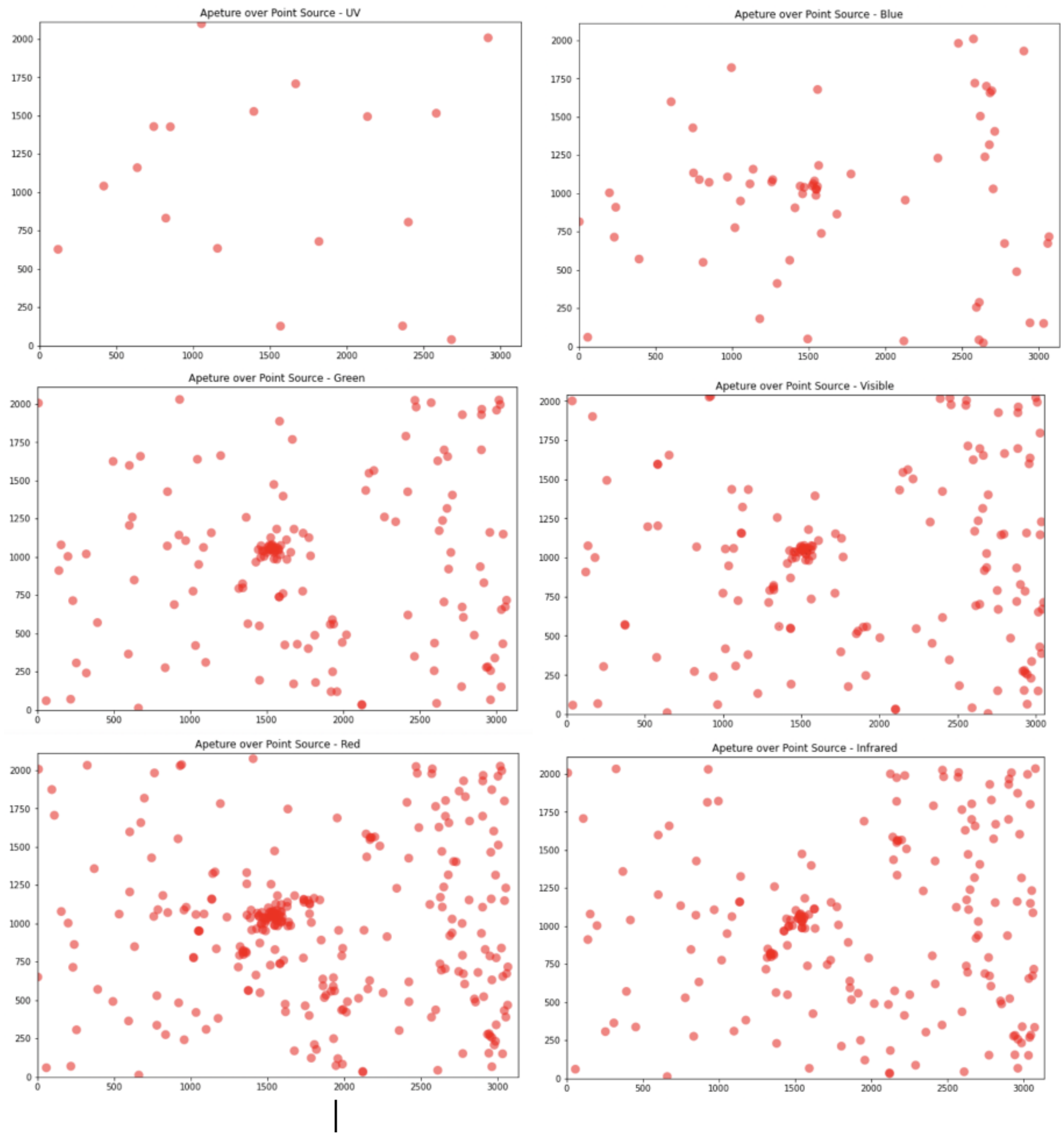

FIG. 7: NGC 2070 Aperture Photometry Plots:

Aperture Over Point Sources Detected in six different filter bands: From left to right, top to bottom; Bessel UV; Bessel Blue; SDSS Green; SDSS Visible: SDSS Red; and SDSS Infrared. Point sources for NGC 2070 were primarily detected in the green, red, and infrared bands. Blue point source detections were significantly reduced, and very few UV point sources were detected.

Color Magnitude Diagrams

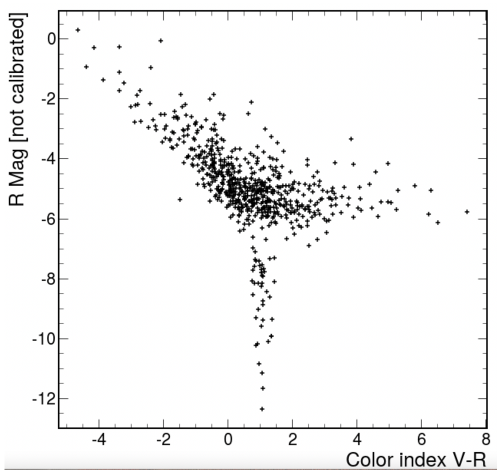

FIG. 8: Messier 2 Color-Magnitude Diagram (V-R)

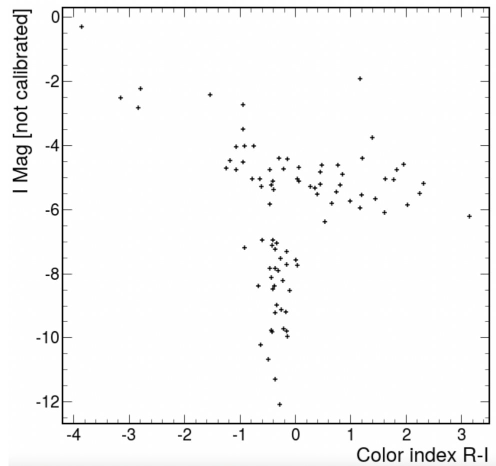

FIG. 9: Messier 2 Color-Magnitude Diagram (R-I)

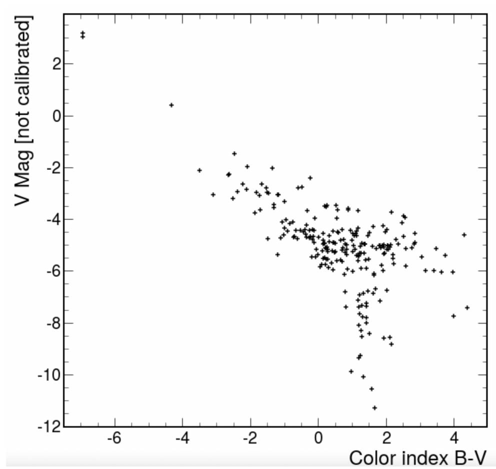

FIG. 10: Messier 2 Color-Magnitude Diagram (B-V)

Messier 2 Color-Magnitude diagrams were prepared in three color indices (FIGs. 9-12 above)(Insufficient point source detection in the UV precluded a U-V plot). FIG. 9 illustrates the majority star detection in the redder, older stars. The B-V plot in FIG. 10 illustrates a lack of stars in the upper part of the main sequence.

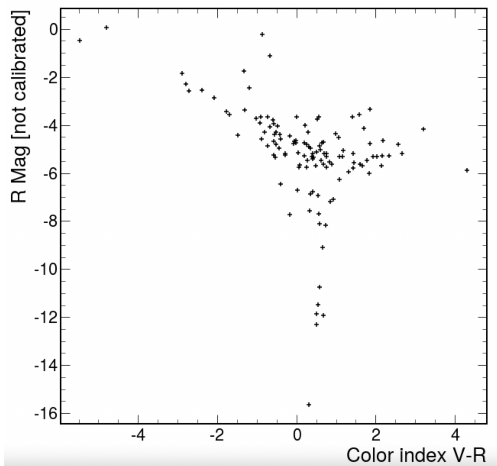

FIG. 11: Beehive Cluster Color-Magnitude Diagram (V-R)

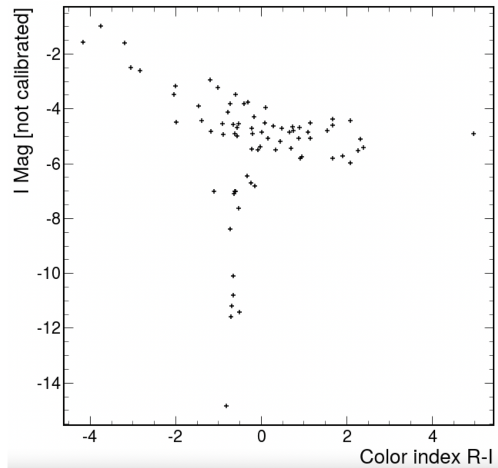

FIG. 12: Beehive Cluster Color-Magnitude Diagram (R-I)

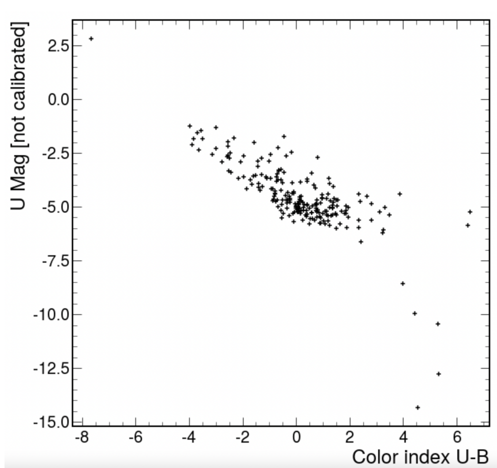

FIG. 13: Beehive Cluster Color-Magnitude Diagram (U-B)

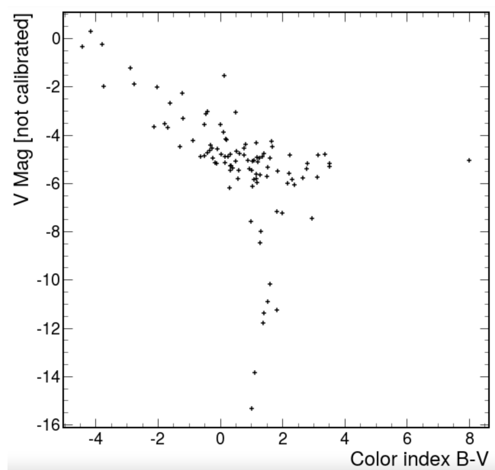

FIG. 14: Beehive Cluster Color-Magnitude Diagram (B-V)

Beehive Cluster Color-Magnitude Diagrams were prepared in four color indices (FIGs. 12-15 above). FIGs 12-15 show similar numbers of stars detected across the color indices. The B-V plot in FIG. 15 illustrates a well populated upper main sequence.

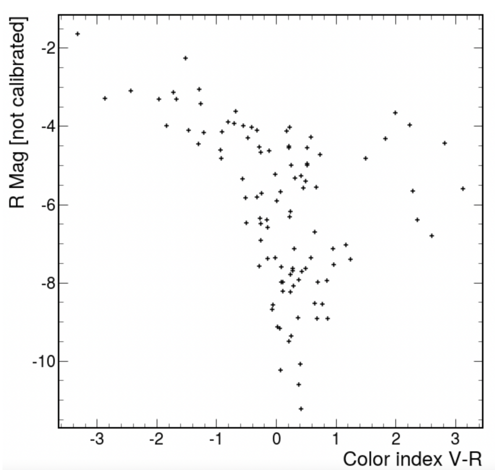

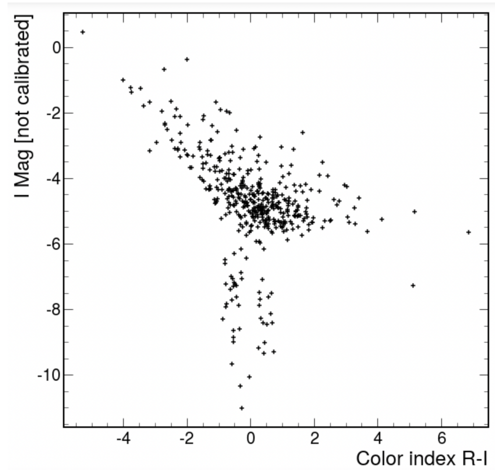

FIG. 15: NGC 2070
Color-Magnitude Diagram (V-R)

FIG. 16: NGC 2070
Color-Magnitude Diagram (R-I)

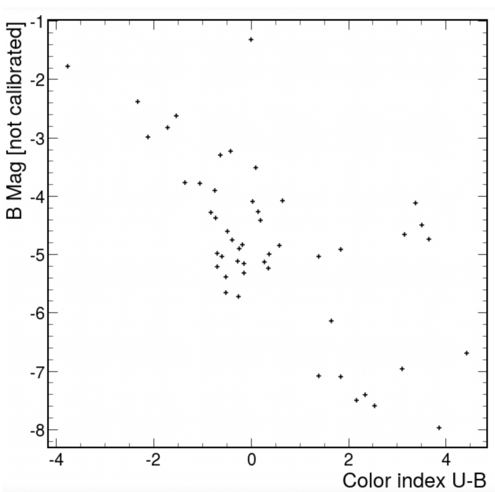

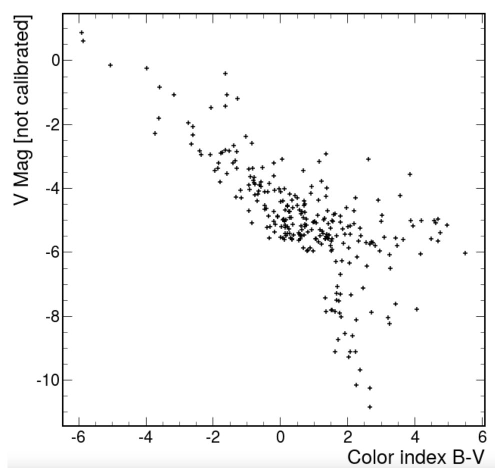

FIG. 17: NGC 2070
Color-Magnitude Diagram (U-B))

FIG. 18: NGC 2070
Color-Magnitude Diagram (B-V)

NGC 2070 Color-Magnitude Diagrams were prepared in four color indices (FIGs. 16-19 above). Fig. 17 illustrates the large numbers of point sources detections in the red and infrared. Fig 19. shows a well populated middle main sequence, and a less well populated upper main sequence.

ERROR ANALYSIS

Magnitude Calibration

The CMD plots as presented are uncalibrated. All attempts were made to find reference stars, and incorporate them into the code, however, a number of issues hindered this process. Four reference stars with x,y coordinates were found for each cluster image, and their magnitudes in the V band obtained from the Gaia catalogue. These reference stars were the four brightest stars in the visible band from each cluster image. Messier 2 reference stars were in the order 10th magnitude stars; Beehive Cluster reference stars were in the order 6th magnitude stars; and NGC 2070 reference stars were fainter, in the order 20th magnitude. When calibrating the Python code magnitudes, non-sensical magnitude stars appeared in color magnitude plots. It is unclear to date how to resolve this issue. It is most likely that when attempting to locate the reference stars from within the Python code, incorrect stars were found, with inappropriate magnitude applied. What is needed is a highly accurate method of position correspondence between reference stars obtained from RA and Dec coordinates in a catalogue, with x,y coordinates of point sources detected by the Python code.

Interloper Stars

The problem of foreground and backgound stars contaminating the actual 'cluster stars' is significant. For Messier 2 and the Beehive cluster the issue is not as obvious, but for the NGC 2070 cluster, the stars populating the CMD are undoubtedly not the stars of the central cluster, but rather they are stars in the surrounding Tarantula Nebula.

Aperture Choice

The use of a chosen aperture to determine a point source flux introduces some degree of error into the magnitude determinations. A number of different aperture values were chosen (r=15, r=5, and r=4), which altered the flux magnitudes but did not significantly affect the overall number of point sources detected, or the general pattern of the CMDs. This would, I propose, affect the position of the main sequence relative to a calibrated magnitude scale.

A second issue the aperture method unavoidably introduces is the accuracy of detections in overcrowded areas, such as the center of the densely packed Messier 2, and globular clusters more generally.

Signal to Noise

Signal to Noise calculations were carried out in Python using CCD and telescope specifications (see Table II, p8). A background Flux of 0.01 and an integration time of 5 seconds was used to calculate signal to noise across a range of magnitudes from m=0 to m=30 (see Appendix B for Python calculations). Results are as follows:

TABLE III: Signal to Noise for magnitude (0-30).

Magnitude 0	80066
Magnitude 5	8006
Magnitude 10	800
Magnitude 15	78
Magnitude 20	4
Magnitude 25	0
Magnitude 30	0

Messier 2 reference stars were in the 10th magnitude range. We estimate a range of magnitudes for the M2 cluster between 10 and 20, and a corresponding signal to noise range for Messier 2 800-4. This is a reasonable S/N, however it would be improved by stacking 10 to 20 images before processing.

Beehive Cluster reference stars were in the 6th magnitude range. We estimate a range of magnitudes for the M2 cluster between 6 and 15, and a corresponding signal to noise range for Beehive Cluster of approximately 8000-78. This is a better S/N ratio than for Messier 2, however it would also be improved by stacking images before processing.

NGC 2070 Cluster reference stars were in the 20th magnitude range, and as such we estimate very low signal to noise below 4 for these images, and thus the data has too much noise to be useful.

DISCUSSION

Messier 2

The Messier 2 cluster is large, centrally dense, globular cluster as shown in the base and Tricolor images FIG. 3 and FIG 4. Point source detection in the Cluster was greatest in the red filter, as illustrated by the aperture photometry plots in FIG. 5. Color magnitude diagrams for Messier 2 (FIGs. 8-10) indicate a higher proportion of stars in the red part of the spectrum. With very little detection of point sources in the blue and UV, as such no U-V plot was produced. It is possible that a longer integration time (than 5 seconds) in the blue and UV filters would be appropriate due to the lower photon detection in these filters (pers. com. Dr Lubin). However, as Messier 2 is estimated to be more than 13 Gyr old, it is sensical to see a larger proportion of point sources in the red filter. These very old clusters are described in the literature as 'red and dead' (Corroll and Ostlie 2017). The B-V plot in FIG. 10 illustrates a lack of stars towards the upper left corner of the plot, representing the upper part of the main sequence. We would expect to see this section of the main sequence devoid of stars in an old cluster like Messier 2. We may compare our plot with the following figure from the literature that illustrates the color magnitude relationship for Messier 2 (V-R), where the upper part of the main sequence has turned off.

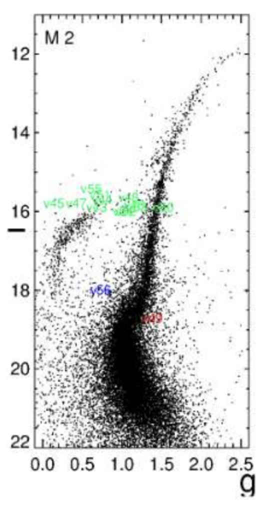

FIG. 19: Messier 2 Color Magnitude Diagram (V-R), NoirLab 2016

Beehive Cluster

Beehive Cluster Color-Magnitude Diagrams were prepared in four color indices (FIGs. 12-15, p14). The figures show similar numbers of stars detected across the color indices. The B-V plot in FIG. 15 illustrates a well populated upper main sequence, which we would expect to see in an intermediate age cluster like Beehive (900 Myr). We may compare with Fig. 20 below, a color magnitude diagram from the literature prepared by StarObserver with photometric data obtained by Johnson (1956). Our plots are consistent with the well populated diagonal main sequence indicated in FIG 20, though the trend is not quite as clear.

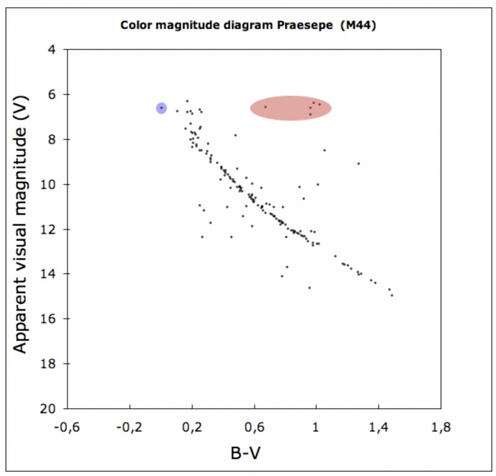

FIG. 20: Beehive CMD

NGC 2070

The distance to NGC 2070 of 157,000 Ly, three times as far as Messier 2, ensured that the central star cluster was essentially unresolvable with the 0.4 meter telescope. Upon reflection, Walker (1956) makes note of the importance of choosing nearby star clusters, so that both bright *and* faint stars can be detected. He also notes that there must be minimum emission nebulosity in order to detect the fainter stars. The Tarantula Nebula dominates our images, and, in fact we are not detecting the central star cluster, but rather the nebula and foreground stars. Coupling this with the very low signal to noise for the point sources in these images, we propose an inconclusive result for the NGC 2070 star cluster.

Conclusion

The photometric analysis of Messier 2, Beehive Cluster, and NGC 2070 from data obtained by the Las Cumbres Observatory (LCO) 0.4 m telescope produced varying results across the three very different clusters.

The Messier 2 base images were well enough resolved to produce a good Tricolor image as well as data for color magnitude diagrams with a reasonable signal to noise ratio. The process of producing the color magnitude diagrams highlighted significant challenges and provided much room for error. As a result, the interpretation of the color magnitude diagrams was cautiously made, with comparisons to color magnitude diagrams in the literature. The resulting plots did appear sensical, and are consistent with a very old globular cluster. However, there is certainly much room for improvement of the photometric software, as well as a more nuanced approach to the choice of integration time across the filter range.

The Beehive Cluster base and Tricolor images clearly present a younger open cluster, and the data for the color magnitude diagrams had a good signal to noise ratio. It is therefor more reliable than the Messier 2 data. The well populated entire main sequence for the Beehive Cluster is consistent with its estimated intermediate age of 900 Myr.

The base and Tricolor images of NGC 2070, while amongst the most striking of all the images in the study, were in fact the least useful for photometric analysis. The three-fold further distance to this cluster (than Messier) ensured that the telescope was not able to resolve the central star cluster amidst the Tarantula Nebula. The point sources detected were of foreground stars and nebulosity. The very low signal to noise values for the NGC 2070 data precluded us from providing any interpretation of the color magnitude diagrams.

In conclusion, this photometric analysis was a worthwhile first stage investigation into using aperture photometry to analyse photometric data from a professional telescope. Further investigations would provide an opportunity to choose more appropriate (closer, open) clusters to analyse, and to test different integration times across different filters. With these improvements, as well as those in the software, worthwhile photometric analyses could be made, which would undoubtedly contribute to theories of stella and galactic evolution.

Bibliography

Aplegen, 2011, Astronomical Instruments – STL 6303 Typical Specifications, Santa Barbara Instrument Group, viewed on 11/21/2022, viewed at: https://www.virtualtelescope.eu/wordpress/wp-content/uploads/2012/10/STL6303$_{s}pecs_{7}.12.11.pdf?x$67046

Carroll and Ostlie (2017), Introduction to Modern Astrophysics, 2nd edn, Cambridge University Press, United Kingdom.

De Brito Silva, D, et.al. 2022, J-PLUS: Detecting and studying extragalactic globular clusters The case of NGC 1023, Astronomy and Astrophysics, vol. 664, id.A129, 22 pp, viewed on 11/13/2022, viewed at: https://www.aanda.org/articles/aa/pdf/2022/08/aa42402-21.pdf

Johnson H.L., Praesepe, magnitudes and colors, 1952ApJ...116..640J. (2018) M44 Praesepe Color Magnitude Diagram, From StarObserver Website (produced from data by Johnson, H.L (1952) Praesepe: Magnitudes and Colors, Astrophysical Journal, vol. 116, p.640, viewed on 11/28/22, viewed at: http://www.starobserver.eu/articles/M44praesepe/

Lodieu, N, Pe rez-Garrido, A, Smart, L, and Silvotti, R, 2019, A 5D view of the Per, Pleiades, and Praesepe clusters, Astronomy and Astrophysics, vol. 628, id.A66, 26 pp, viewed on 11/13/2022, viewed at: https://arxiv.org/pdf/1906.03924.pdf

Lubin, P, 2022, Notes for PHYS134L – Observational Astrophysics, University of California, Santa Barbara, viewed on 10/01/2022, viewed at: https://www.deepspace.ucsb.edu/wp-content/uploads/2022/09/134-Notes-10-22-1.pdf

NoirLab (2016) The color-magnitude diagrams of the four globular clusters M2, M10, M80 and NGC 1261, produced from the SAM data, viewed on 11/30/22, viewed at: https://noirlab.edu/science/images/SAM$_{p}hotometry_{G}Cs_{S}alinas_{e}tal_{2}$016

Richmond, M. no date, 'Interpreting the H-R Diagram of stella clusters', Rochester University of Technology, New York, viewed on 10/12/2022, viewed at: http://spiff.rit.edu/classes/phys230/lectur

Sanner, J. M et al. (2000) Photometric and kinematic studies of open star clusters. II.

NGC 1960 (M 36) and NGC 2194, Astronomy and Astrophysics, v.357, p.471-483, viewed on 11/25/22, viewed at:https://arxiv.org/abs/astro-ph/0003327

Taylor, J.R. (1997) An Introduction to Error Analysis, 2nd edn. University Science Books, Sausalito, California.

Walker, M, 1956 Studies of Extremely Young Clusters. I. NGC 2264, Astrophysical Journal Supplement, vol. 2, p 365, viewed on: 10/12/2022, viewed at: https://articles.adsabs.harvard.edu/pdf/1956

Aurieie, M and Cordoni, J.P. (1983) The color-magnitude diagram for stars in the central pat of the globular cluster NGC 7089 (M2), Astronomy and Astrophysics Supplement Series, vol.51, pp 135-142, viewed on 11/28/22, viewed at: https://articles.adsabs.harvard.edu/full/1983A

APPENDIX B

```
import os
import numpy as np
import math
import matplotlib.pyplot as plt
#Define parameters
NR = 13.5
iDC = 0.3
Qe = 0.68
Om = 0.326
A = 1257
Eps = 0.5
Time = 5
Ae = 427.38 # Effective Area
FB = 0.01   # Background Flux
F0 = 3e6    #Flux from a 0th magnitude star
F5 = 3e4    #FLux from a 5th magnitude star
F10 = 300   #Flux from a 10th magnitude star
F15 = 3     #Flux from a 15th magnitude star
F20 = 0.03  #Flux from a 20th magnitude star
F25 = 3e-4  #Flux from a 25th magnitude star
F30 = 3e-6  #Flux from a 30th magnitude star
NT0 = (F0*Ae) + (iDC) + (FB*Ae*Om) #Time Dependant noise
SN0 = (F0*Ae*Time) /math.sqrt (NR**2 + Time*NT0)
NT5 = (F5*Ae) + (iDC) + (FB*Ae*Om) #Time Dependant noise
SN5 = (F5*Ae*Time) /math.sqrt (NR**2 + Time*NT5)
NT10 = (F10*Ae) + (iDC) + (FB*Ae*Om) #Time Dependant noise
SN10 = (F10*Ae*Time) /math.sqrt (NR**2 + Time*NT10)
NT15 = (F15*Ae) + (iDC) + (FB*Ae*Om) #Time Dependant noise
SN15 = (F15*Ae*Time) /math.sqrt (NR**2 + Time*NT15)
NT20 = (F20*Ae) + (iDC) + (FB*Ae*Om) #Time Dependant noise
SN20 = (F20*Ae*Time) /math.sqrt (NR**2 + Time*NT20)
NT25 = (F25*Ae) + (iDC) + (FB*Ae*Om) #Time Dependant noise
SN25 = (F25*Ae*Time) /math.sqrt (NR**2 + Time*NT25)
NT30 = (F30*Ae) + (iDC) + (FB*Ae*Om) #Time Dependant noise
SN30 = (F30*Ae*Time) /math.sqrt (NR**2 + Time*NT30)
print (SN0)
print (SN5)
print (SN10)
print (SN15)
print (SN20)
print (SN25)
print (SN30)
```

```
80066.84588069966
8006.672797378033
800.5493991170183
78.9017968079509
4.015927752096019
0.046342863368957786
0.0004641990585247431
```

FIG. 21: Signal To Noise Python Calculations